Journal Homepage: https://dergipark.org.tr/tr/pub/isibted

Isı Bilimi ve Tekniği Dergisi

Archive: https://tibtd.org.tr/dergi

Effect of BioPCM-Integrated Building Components on Diurnal Heating-Cooling Rates and Local Thermal Sensations

Neslihan Türkmenoğlu BAYRAKTAR [1,] *, Merve Kılınç GİLİSIRALIOĞLU [1]

[1] *Kocaeli Üniversitesi, Mimarlık ve Tasarım Fakültesi, Mimarlık Bölümü, İzmit, 41300, Kocaeli, Türkiye*

A R T I C L E I N F O

2025, vol. 45, no.2, pp. 296-316

doi: 10.47480/isibted.1668591

Research Article
Received: 31 March 2025
Accepted: 19 August 2025

* *Corresponding Author*
e-mail:
nturkmenoglu@kocaeli.edu.tr

Keywords:
BioPCM
Thermal comfort
Heating-cooling rate
Local physiological stress
Transition period

ORCID Numbers in author order:
0000-0003-0059-5721
0000-0002-5390-843X

A B S T R A C T

Phase change materials (PCMs) reduce heating-cooling loads while improving thermal comfort in buildings. However, instead of applying it to the total building envelope, using it on different building components may increase energy consumption and local thermal discomfort. Unlike previous studies applying PCM across all building components, this study uniquely investigates the effects of integrating BioPCM into individual components, each with an equal PCM-applied surface area, considering their solar exposure due to orientation. By controlling both PCM area and orientation, this study provides a framework to isolate and quantify their combined effects on building thermal performance. Diurnal heating-cooling rates and thermal comfort are evaluated via predicted mean vote (PMV) maps and physiological stress grades at nine locations over five time intervals, focusing on hottest and transition periods under temperate climate conditions. Additionally, surface temperatures and heat storage rate variations were analyzed to characterize diurnal behavior. Results showed that all BioPCM scenarios mitigated cooling, with roof integration reaching a 25% reduction. Only east-west walls and roof notably reduced heating, with modest enhancements to sensation. The south wall minimized thermal stress, while the East wall still exhibited high stress grades during transitions. These limited effects were primarily due to insufficient BioPCM-applied area equally allocated, constraining full indoor thermal regulation potential.

BioPCM Entegreli Bina Bileşenlerinin Günlük Isıtma Soğutma Oranları ve Lokal Isıl Hissiyatlara Etkisi

M A K A L E B İ L G İ S İ

Anahtar Kelimeler:
BioPCM
Isıl konfor
Isıtma-soğutma oranı
Lokal fizyolojik stres
Geçiş dönemi

Ö Z E T

Faz değiştiren malzemeler (FDM), ısıtma, soğutma yüklerini azaltırken ısıl konfor koşullarını iyileştirir. Ancak, bu malzemelerin tüm bina yüzeylerine uygulamasından ziyade, farklı yapı bileşenlerine tekil olarak uygulanması, enerji tüketimi ve lokal ısıl konforsuzluğu arttırabilir. Tüm bina bileşenlerine FDM uygulanan önceki çalışmalardan farklı şekilde, bu çalışma, her biri eşit FDM uygulanmış yüzey alanına sahip bina bileşenlerine BioPCM entegrasyonunun etkilerini, yönelime bağlı güneş ışınımına maruz kalma koşullarını dikkate alarak incelemektedir. Çalışma FDM uygulama alanı ile yönelimi eşzamanlı olarak kontrol ederek, bina ısıl performansı üzerindeki birleşik etkilerini izole etmeye ve niceliksel olarak değerlendirmeye yönelik özgün bir çerçeve sunmaktadır. Nemli-ılıman iklim koşullarında en sıcak ve geçiş dönemlerine odaklanılarak, gündüz saatlerindeki ısıtma-soğutma oranları ile lokal ısıl konfor seviyeleri, dokuz noktada, beş farklı zaman aralığında elde edilen PMV (tahmini ortalama oy) haritaları ve fizyolojik stres puanlamaları ile değerlendirilmiştir. Ayrıca, her bileşenin gündüz ısıl davranışını karakterize etmek amacıyla yüzey sıcaklıkları ve ısı depolama oranlarındaki değişimler analiz edilmiştir. Sonuçlar, BioPCM senaryolarının soğutma yüklerini azalttığını, çatı enetegrasyonun ise %25'e varan azalma sğladığını göstermiştir. Sadece doğu-batı duvarları ve çatı uygulamasında ısıtma oranları azalırken, ısıl hissiyatta sınırlı iyileşmeler kaydedilmiştir. Güney duvarı ısıl stresi en az seviyeye indirirken, doğu duvarı geçiş dönemlerinde yüksek lokal stres üretmiştir. Bu sınırlı etkilerin nedeni, BioPCM'in her bileşene eşit ancak yetersiz yüzey alanı ile uygulanması olup, iç ısıl ortamı dengeleme potansiyelinin tam olarak sağlanamamasına dayanmaktadır.

NOMENCLATURE

MBE (%)	Mean bias error
M_i	Measurement result
S_i	Simulation result
n	Number of measurements
$\overline{M}$	Average of measurements
CV(RMSE)%	The coefficient of variation of the root square error, as the percentage of the mean observed value
C_p	Specific heat capacity ($kJkg^{-1}K^{-1}$)
ρ	Density (kg/m^3)
Δx	Thickness among nodes(m)
T	Temperature (^{0} C)
J+1	New time step
i+1	The adjacent node to the interior of the construction
Δt	Time step
k_w	The thermal conductivity of the interface between nodes i and i + 1(W/mK)
k_e	The thermal conductivity of the interface between the nodes i and i–1
$h_{i,\,old}$	Enthalpy at the old condition (J/kg)
$h_{i,\,new}$	Enthalpy in the new condition(J/kg)
$T_{i,\,old}$	Temperature at the old condition (^{0}C)
$T_{i,\,new}$	Temperature at the new condition (^{0}C)
DI	Discomfort Index
T_d	Dry bulb temperature (^{0}C)
T_w	Wet bulb temperature (^{0}C)
x'	Normalized value
x	Original value
$x_{\,min}$	Minimum value
$x_{\,max}$	Maximum value
$h_{i,\,old}$	Enthalpy at the old condition (J/kg)
$h_{i,\,new}$	Enthalpy in the new condition(J/kg)
$T_{i,\,old}$	Temperature at the old condition (^{0}C)
$T_{i,\,new}$	Temperature at the new condition (^{0}C)

INTRODUCTION

In recent years, innovative approaches in the construction sector have emerged in line with the main objectives, including using renewable energy sources, reducing energy demands and consumption, and providing energy conversion and conservation with appropriate, new-generation energy storage technologies. Among these, the latent heat storage technique is gaining importance due to its potential to improve building heating and cooling efficiency.

Dinçer and Rosen (2011) emphasize that latent heat storage systems have become a preferred mechanism for enhancing energy performance due to their ability to store heat during peak heat supply for later use when needed. In a daily cycle, the benefits of renewable energy sources are unstable, and a need arises for supplementary systems to balance supply and demand. Therefore, thermal energy storage systems, classified as thermochemical, sensible, and latent heat storage, help balance supply and demand without the need for fossil fuels when the effects of renewable energy sources are insufficient to meet cooling and heating requirements. PCMs, as latent heat storage materials, offer advantages in reducing energy consumption and regulating temperature, enhancing thermal comfort with thinner layers and higher heat storage capacity than materials storing sensible heat (Kuznik et al., 2010; Alharbey et al., 2022). Building PCMs can be applied through direct incorporation, immersion, macro/microencapsulation, and shape stabilization, providing versatility in their integration into building components (Fig. 1).

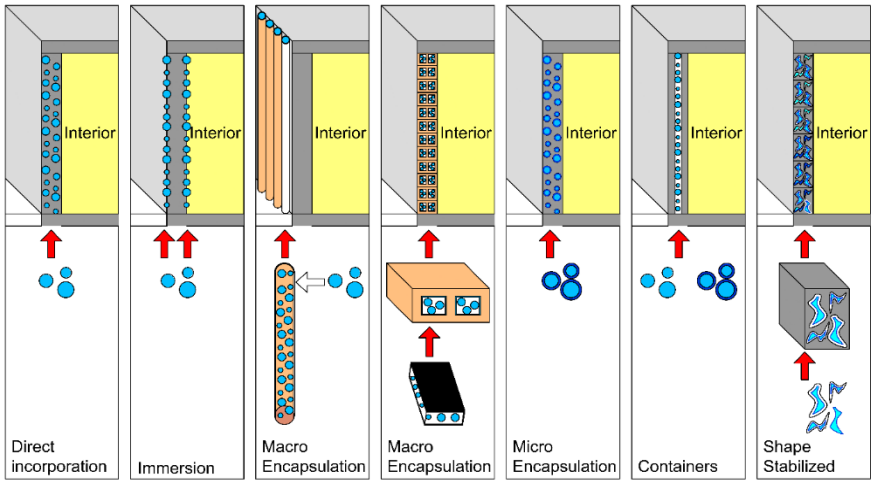

Fig. 1. Different types of PCM application methods (Rathore & Shukla, 2019; Casini, 2016; Socaciu, 2012; Tunçbilek et al. 2020; Vincente and Silva 2014; Cardenas-Ramirez et al. 2020)

The studies on PCM application in buildings primarily focus on selecting effective PCM types, considering appropriate melting temperature range, thickness, layout, and location in different climates. De Masi et al. (2020) identified the melting temperature, latent heat capacity, specific heat in liquid and solid phases, thermal conductivity, and charge/discharge capability as the critical characteristics of PCMs. The study by Alharbey et al. (2022) mentions that a melting-freezing temperature range of PCMs is an essential issue for its efficiency in reducing energy loads and enhancing thermal comfort by maintaining stable operative temperatures.

Some studies by Alharbey et al. (2022), Saffari et al. (2016), and Ahangari and Maerefat (2018) focus on the placement of the PCMs by mentioning that the selection of appropriate building components, such as walls, roofs, and interior partitions, for PCM application, is a critical issue, as the performance of PCMs in improving thermal inertia and indoor thermal comfort varies depending on their exposure to external climatic conditions. Studies by Figueiredo et al. (2017), Bohorquez-Ordenes et al. (2021), Qu et al. (2021), and Alharbey et al. (2022) have emphasized that applying PCMs to building components exposed to intense solar radiation enhances heat storage capacity, dampens temperature fluctuations, and improves thermal comfort.

These studies show that direct solar radiation is a crucial criterion for PCM applications, providing thermal regulation benefits. External climatic conditions lead to seasonal variations in PCM effectiveness in reducing radiant asymmetry, energy consumption, and temperature oscillations. PCMs enhance local thermal comfort by delaying peak thermal loads and providing stable temperatures near their phase change points (Rathore & Shukla, 2019). However, with higher exposure to solar radiation, PCM applications on the roof and southern walls may cause the PCM to remain in a long-term liquid form, leading to increased surface temperatures, radiant asymmetry, and reduced performance. While affecting heating and cooling rates, PCMs on different building elements may create uncomfortable thermal conditions for occupants during peak and transition periods due to radiant asymmetry. Ngahana and Atariku (2016) evaluated the effect of PCM on differently oriented walls in their experimental and simulation-based study on lightweight constructions, focusing on thermal comfort by analyzing indoor temperature stabilization and the reduction of temperature peak performance. They found results comparable to winter outcomes without separately focusing on the transition period. Ahangari and Maerefat (2018) examined the regional variations in operative temperatures influenced by radiant temperature, indoor air movement, and solar radiation. Their study considered the effect of PCM on different building elements on thermal comfort by the Fanger method in various climates, with only focusing focused mainly on radiation heat transfer between inner surfaces and occupants without examining the impact of different PCM-integrated building components, such as variously oriented outer walls, partitions, and roofs, specifically. Although some studies, such as Qu et al. (2021) and Kuznik et al. (2010), focus on PCM layer layout, type, and thickness affecting energy consumption in peak periods, the gap in the literature regarding the effects of PCMs on various buildings components on not only energy savings but also local thermal sensations of the occupants particularly in transition periods, cannot be sufficiently addressed.

The novelty of this research is its focus on the diurnal variation of energy savings and thermal sensations of occupants due to the application of an equal amount of BioPCM on different building elements, such as outer walls, partitions, and the roof for each scenario instead of covering all surfaces for comparison among the cases, during the peak hottest and the transition periods under temperate climatic conditions. The study examines the impact of bio-phase change material (BioPCM) placement on interior surfaces, focusing on variations in heating and cooling rates and occupants' local indoor thermal comfort sensations in diurnal, five-time intervals, considering both heat and cold stresses. The results are normalized to evaluate the effectiveness of each scenario in reducing cold-heat stress hours and heating-cooling rates during the typical hottest day of August and November, the usual day of the transition period.

METHODOLOGY

An environmentally friendly BioPCM was assumed to be applied uniformly to the outer walls of the South, West, and East, as well as the South partition and the roof of the lightweight, single-floor campus building in each scenario. The building is located in Kocaeli, Türkiye, which has a temperate climate. To preserve the building facade, macro-encapsulated, bio-based PCM sheets supported by gypsum board are applied on the interior surface, complementing the existing insulation on the outer surface. Thermal stress levels at nine indoor reference locations were analyzed at five different time intervals on August 21 and November 21, representing typical days of the hottest and transition periods. November was selected to assess the potential risks of PCM during temperate seasons and to capture the changes that follow the peak period, an often overlooked season considered less risky. Six scenarios are examined for their effects on thermal comfort using PMV indices derived from Energyplus analysis with the Fanger method (Energyplus, 2022). Spatial variation plots of PMV values and physiological stress grades compare the effects of PCM on thermal comfort at nine specific locations and five intervals during the hottest and transition periods. The scenarios are assessed based on their effectiveness in reducing heating and cooling rates and mitigating thermal stress using the min-max normalization method. The study presents variations in solar radiation and heat storage on PCM-integrated walls, considering the shading effects from surrounding buildings. Throughout the study, the assumptions on the building geometry, occupancy schedule, internal gains, equipment, and HVAC system settings remained constant variables to ensure comparability of the scenarios. The PCM applied surface area was fixed at 53.4 m2 for each scenario, which was determined due to the shortest façade dimensions of the rectangular planned building. Windows were assumed to be closed during occupancy hours, with no night ventilation integration. Indoor air velocity was considered negligible, as measurements consistently showed velocities below 0.1 m/s. A basic enthalpy-temperature model was used based on the manufacturer's limited data.

Building and Site Characteristics

The Kocaeli University Anıtpark Campus in Kocaeli, Türkiye, comprises four block structures in a central, densely residential district. The "MTF" design atelier building considered in this study is a 284 m^2 single-story, lightweight structure (Fig. 2). It serves as a drawing atelier and a classroom for theoretical lessons. The building has three thermal zones with openings on the West and east with 20% transparency levels. The atelier is under the shading effects of surrounding buildings.

Fig. 2. Atelier building in Kocaeli University, Anıtpark campus in Kocaeli, Türkiye

Climate

Outdoor Climate Data

Kocaeli, within the 3rd degree day climate region according to the standard TS 825 "Thermal Insulation Requirements for Buildings," presents temperate climatic zone characteristics (TS 825, 2025). Simulations were conducted with Meteorological data files based on actual atmospheric conditions obtained from

the Turkish State Meteorological Center. The IWEC (International Weather for Energy Calculations) weather file was generated for Kocaeli for the typical days of August, the hottest, and November, as the transition period. The maximum, minimum, and average hourly outdoor air temperatures for each month were calculated using 4-year weather data (2018-2020) obtained from the Kocaeli weather station (Station ID:17066) (Fig. 3a). The study focused on typical days in August and November, selected based on their degree-day totals. November presented the lowest heating degree days [HDD] as a transitional period. August presented the highest cooling degree days [CDD] over the four years (Turkish State Meteorological Service 2024) (Fig.3b). The selection of November and August 21 as reference typical days lies in the similarity of the calculated monthly and four-year mean outside temperature data of these days (Fig. 4). According to the meteorological data, the outside temperatures at occupancy periods changed between 28.2 and 25.8 ^{0}C on August 21, 2020.

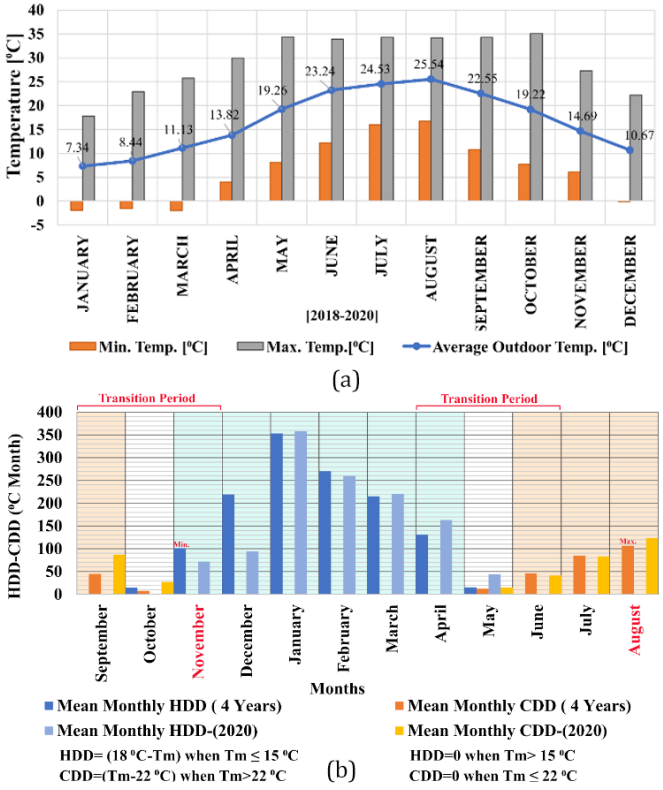

Fig. 3. a-Monthly outdoor temperatures- Meteorological data [2018-2019]. **b**-Heating Degree Day [HDD]- Cooling Degree Day [CDD] variations in Kocaeli-(Turkish State Meteorological Service 2024)

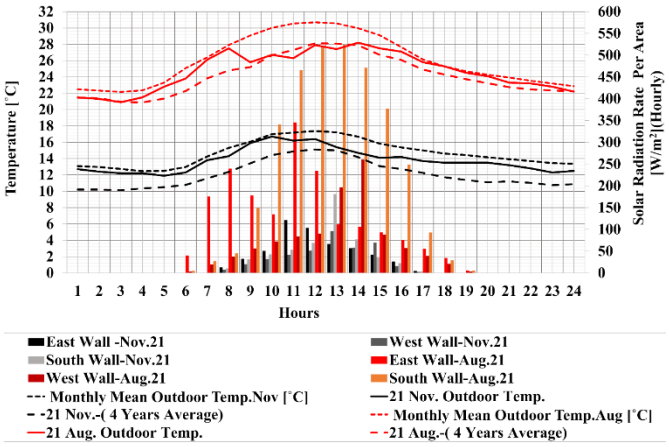

Fig. 4. Wall outside face incident solar rate per area and outdoor temperatures

Indoor Airflow and Temperature Measurements

"Cem DT-171" and Extech RHT 10 temperature-humidity dataloggers, both with an accuracy of ±1.0°C (-10 to 40°C), were positioned at nine reference points to measure indoor temperatures, including points in the middle of the space and close to walls and windows, where students typically sit. Indoor airflow velocities are measured with Testo 435 with a measuring rate of 0-20 m/s and ±(0.03 m/s +5% of mv) accuracy (Fig. 5). Interior mean temperatures at all locations change between 24.32-31.25 ^{0}C, with higher values than outdoor mean temperatures on the August reference day during occupied hours except 09:00-11:00. Measurement results at locations c1, c2, and c3 provided lower temperature values than those outdoors on reference days. The highest mean temperature was at "w3" on the northwest. At the same time, the lowest value was obtained at "c2" in the center of the zone between 09:00 and 13:00. Lower temperature values approaching thermal comfort conditions occurred at all locations during the morning hours. The highest values are measured during the afternoon, from 14:00 to 17:00, at all locations.

Fig.5. The locations of the indoor and outdoor measurement equipment

Temperature oscillation is highest with a maximum temperature difference of 4.64 ^{0}C between morning and afternoon at "e1"-on the southeast. At night, the interior temperature variation is around 26.58-27.21^{0}C. The variations of measured temperatures at locations at all time intervals of occupancy are low. The outside temperatures on the November reference day are between 13.7 and 16.7 ^{0}C, with temperate climatic conditions during occupancy. Monthly mean temperatures range from 15.01 to 17.38 ^{0}C. Interior measured mean temperatures range from 23.20 to 20.96 ^{0}C between 09:00 and 17:00. Interior temperatures are mostly within comfort ranges without heating during the daytime. The highest temperatures are measured at noon, changing between 22.50 and 23.20 ^{0}C. Daily temperature oscillation is the highest, with a difference of 6.68 ^{0}C at the location "w3"-Northwest.

Simulation Configuration and Materials

Simulation Steps

The 3D building was modeled using DesignBuilder software. Calculations were made with the EnergyPlus energy analysis program to examine the thermal sensation levels of occupants and heating-cooling rates in the building during the transition and hottest typical days. The local meteorological data were

used to update the IWEC climate file for Kocaeli, Türkiye, and used in the simulations.

Outside and interior temperature measurements with complete data and simulation results for the reference condition on November 21, 2019, demonstrate the consistency between the simulation and on-site measurement results. This approach aligns with studies by Berardi and Soudian (2017), Qu et al. (2021), De Masi et al. (2020), and Bejan and Catalina (2016), all of whom similarly calibrated their models using measured data. The measured mean relative humidity during occupancy hours was 67.4%. The accuracy of simulation results is examined using the mean bias error (MBE), Eq.(1), and the variation of RMSE coefficient (CV(RMSE), Eq.(2) by Guideline ASHRAE14. This guideline defines acceptable calibration limits for hourly data as ±10% MBE and ≤30% CVRMSE (hourly; Raftery et al., 2011). Mi represents the measurement results, while Si represents the simulation results. "n" is the number of measurements.

$$MBE(\%) = \left(\frac{\sum M_i - S_i)}{n.\bar{M}}\right) \times 100 \quad (1)$$

$$\mathbf{CV(RMSE)}(\%) = \left(\frac{\sqrt{\frac{\sum(M_i - S_i)^2}{n}}}{\bar{M}}\right) \times \mathbf{100} \quad (2)$$

The calculated MBE (%) is -0.099 %, indicating that measured values are delicately lower than the simulation values. CV(RMSE) is 6.21%, which shows that the simulation results are within an acceptable range. In addition to heating-cooling loads, surface heat transfers at interior and exterior surfaces were calculated with EnergyPlus to analyze heat flow variations and quantify the thermal regulation effects of different PCM application scenarios. Therefore, the "EnergyPlus" IWEC file was created using meteorological data for external temperature, wind, and relative humidity on November 21, 2020, and August 21, 2020, representing reference days for transition and cooling periods, respectively.

This study examines the local PMV values resulting from diurnal changes in surface temperatures and heat storage rates by phase change material application on the interior surfaces of the outer walls, partition, and roof, considering shading effects with other buildings. Total cooling and heating rates and the variation of local Physiological Stress grades of occupants caused by the alternatives with and without PCM are compared for the reference locations in the atelier building. Results are obtained for the classroom zone (Zone 2). Fanger's method for thermal comfort calculations was applied using the Energyplus program.

Interior airflow velocity measurements were conducted with Testo 435. However, all the measured air velocities at 9 locations in the zone were negligibly under 0.1 m/s, creating still conditions (Energyplus, 2022). Angle factor and airflow velocity schedules created with measured airflow velocity input are defined in Energyplus for each of the nine locations. Predicted mean vote levels obtained for all situations are visually depicted with a PMV distribution map to observe the hourly and local variations at 9 locations for transition and hottest period reference typical days for all scenarios concurrently. As a result, the investigation delves into PMV thermal stress levels, effectively capturing both heating and cooling stresses experienced by occupants at different locations. The results of the scenarios are evaluated in terms of reducing heating and cooling total rates and decreasing thermal stress using the min-max normalization method. A higher weight is assigned to the thermal stress reduction capability, similar to the approach in the study of Evola et al. (2013), emphasizing it as the main criterion over energy efficiency.

Simulation Configuration

For each of the six scenarios, phase change material is assumed to be applied to an equal amount of surface area (53.4 m²) on the opaque interior surfaces of the building envelope. The quantity was determined based on the location of the building's shortest facade to compare the performance of different PCM-integrated building components to mitigate energy consumption and provide optimal thermal sensation levels. It is preferred to be applied on the inner surface so that the application on the outer wall surface does not ruin the facade aesthetics.

The reference alternative represents the configuration with no PCM and insulation, originally as it is in the existing building. The second alternative includes a thermal insulation layer on the outer surface. Since applying an insulation layer on the inner surface does not protect the building envelope against the physical environmental factors that act on the building elements, the study excludes cases with insulation on the inner surface of the facade. A bio-based PCM application is assumed to be on the south, west, and east facades, partition walls, and partially in the roof for each scenario separately (Fig. 6).

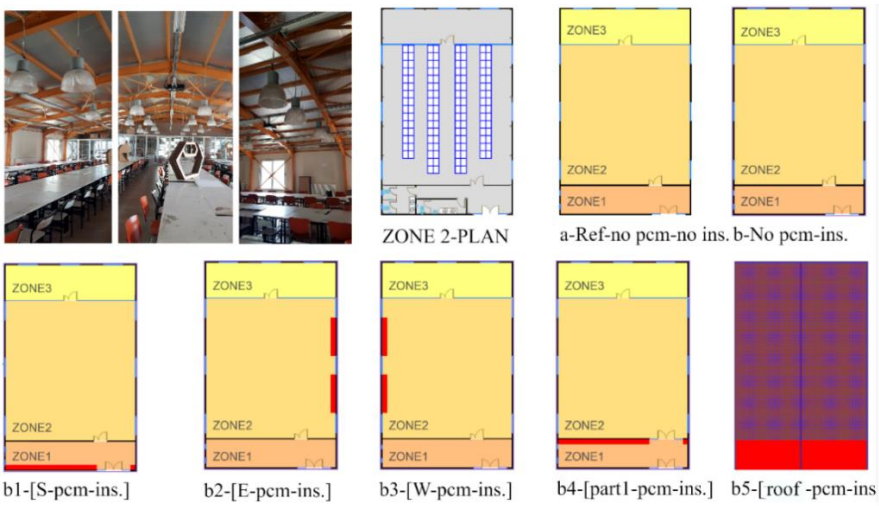

Fig. 6. Simulation alternatives with or without PCM

BioPCM phase change materials are products of plants such as non-food coconut, soybean, palm Kernel, and palm oils (Fabiani et al., 2020). These PCM types are cost-effective and eco-friendly, with lower environmental effects (Aridi & Yehya, 2022; Yadav et al., 2023). Selected BioPCM M182/Q23 has a specific heat of 1970 J/kg-K. The temperature-enthalpy curve (Table 2) and a thickness of 0.0742 m are sourced from the Designbuilder predefined material library (Table 1-2). In the sensitivity analysis Qu et al. (2021) conducted, BioPCM 23 with 7 cm integrated into the indoor surface effectively reduced electricity consumption and increased thermal comfort hours. Commercially available organic-based BioPCM™ products, sold as wrapped into small pockets in a thick plastic foil sheet, are assumed to be attached to the interior surface of one outer wall and on the south part of the roof for each scenario individually (Baniassadi et al. 2019, BioPCM datasheet Q23 2024, Vik et al. 2017). Fig. 7 shows the wall and roof layers of the alternatives with and without BioPCM.

Table 1 Characteristics of BioPCM M182/Q23 (Designbuilder Library)

Characteristics of BioPCM M182/Q23		***Unit***	***Value***
Manufacturer	Phase Change Energy Solutions Inc., USA		
General	Thickness	m	0.0742
	Conductivity	W/m-K	0.2
	Specific Heat	J/kg-K	1970
	Density	kg/m^3	235
Phase Change Properties	Melting temperature	^{0}C	23

Table 2 BioPCM M182/Q23 Temperature-Enthalpy (Designbuilder Library)

Temperature (^{0}C)	***Enthalpy (J/kg)***	***Temperature (^{0}C)***	***Enthalpy (J/kg)***
-20	1	23	201879
0	12	24	236860
10	23058	25	245462
15	32580	27	249194
20	41280	30	254503
21.5	55230	35	258813
22	81820	45	267178
22.5	128509	100	300420

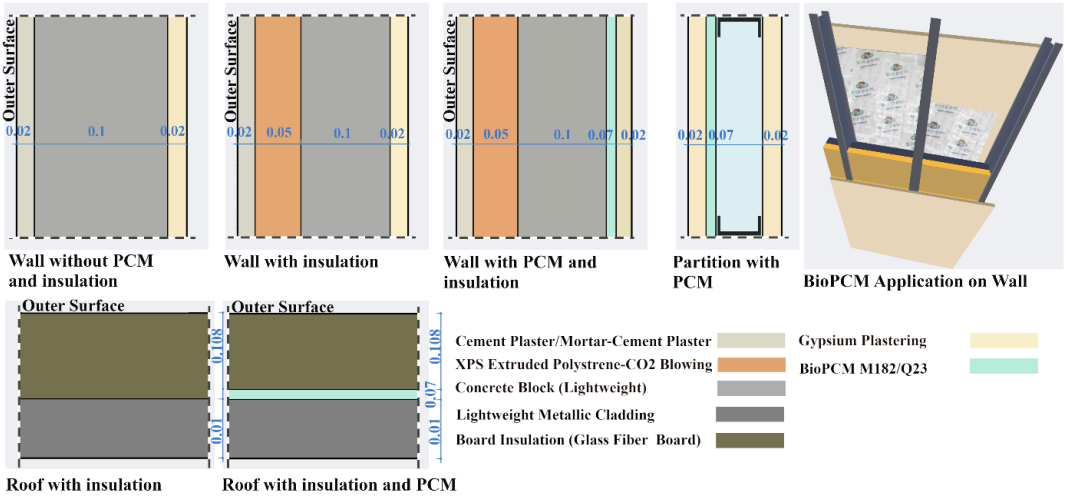

Fig. 7. Wall and roof layers with and without BioPCM. [image for application on wall derived from (BioPCM datasheet Q23 2024)

Students and faculty members, with a total number of 100 people, exist in the atelier between 9:00-12:00 and 13:00-17:00 at the same time during the typical day of the transition period (November) conditions, while there are nine students during the hottest period (August) conditions. The class is empty between 12:00 and 13:00 and after 17:00 in the MTF atelier. The study occasionally neglects issues such as class occupancy reduction in specific periods and the need to open the windows during unoccupied hours. Eleven windows of the atelier are assumed to be closed during the day. The activity level is 144 W/person. Clothing levels are 0.5 Clo for the summer period and 0.9 Clo for the Autumn period. The wall-mounted mono split and two air-conditioner systems supply cooling and heating demands in autumn and summer. The heating and cooling systems were defined with an "ideal load HVAC object" in Energyplus for the simulations. The set point room temperature for the ideal load system is 19 ^{0}C for heating and 26 ^{0}C for cooling. Zone controls, equipment configurations, and ideal load system components are defined instead of modeling a complex HVAC system. District heating and cooling outputs report the energy use data (Energyplus, 2022). The heating and cooling rates were obtained for the hottest and temperate typical days between 01:00-08:00, 09:00-11:00, 12:00-13:00,14:00-17:00, and 18:00-24:00 time intervals. At the same time, the operative temperatures were calculated without the operation of the ideal load system.

A "conduction finite difference" method associated with the enthalpy-temperature function incorporated in "Energyplus" conducts heat transfer calculations with the PCM materials. "EnergyPlus" offers two PCM modeling methods: a "basic method" using the same temperature/enthalpy curve for melting and freezing, and a hysteresis method using distinct curves. Although Berardi and Manca (2017) measured the hysteresis between the melting and the solidification cycles separately, the manufacturer's declared data for BioPCM M182/Q23 was prioritized instead, which is also referred to by Designbuilder. Masi et al. (2020) highlighted that many practical

applications use simplified models due to the lack of detailed data. As the declared data for the selected BioPCM was not thorough enough to define the hysteresis model, considering the practical limitations emphasized by Costanzo et al. (2018) for the actual thickness and the appropriate density of PCM, which affects the accuracy of the modeling, the basic model was preferred to assess PCM performance. The basic model effectively provides the essential thermal properties required for this study and aligns with standard practices in the literature (Costanzo et al., 2018; Wijesuriya et al., 2018).

The method defines each building envelope material with an appropriate number of indoor and outdoor, interior-exterior surfaces, and interface nodes using a fully implicit scheme based on an Adams-Moulton solution approach (Eq.(3) (Energyplus, 2022), where Cp is specific heat capacity (kJkg-1K-1), Δt the time step, ΔX thickness among nodes (m), i is the node being modeled, i+1 is the adjacent node to the interior of the construction, i−1 is the neighboring node to the exterior of the building, j+1 is the new time step, j is the previous time step, Ke is the thermal conductivity of the interface between the nodes i and i−1 (W/mK), Kw is the thermal conductivity of the interface between nodes i and i + 1(W/mK), T is the temperature (^{0}C), ρ is density (kg/m3). In the study, the space discretization value is three, while the relaxation factor is one.

$$C_p \rho \Delta x \frac{T_{i+1}^{j+1} - T_i^{j+1}}{\Delta t} = k_W \frac{T_{i+1}^{j+1} - T_i^{j+1}}{\Delta x} + k_E \frac{T_{i-1}^{j+1} - T_i^{j+1}}{\Delta x} \quad (3)$$

The heat capacity of PCM material is updated with Eq.(4) below as a function of temperature, where Cp represents heat capacity (kJ/kg K), "hi " node enthalpy (kJkg-1) to obtain equivalent specific heat at each time step, hold enthalpy at the old condition (J/kg), "h new" enthalpy in the new condition(J/kg), Tiold temperature at the old condition (^{0}C) and "Ti, new" temperature at the new condition (^{0}C) (Energyplus, 2022).

$$C_p = \frac{h_{i,old} - h_{i,new}}{T_{i,old} - T_{i,new}} \quad (4)$$

RESULTS

A series of comparative scenario analyses based on a simulation campaign was conducted to evaluate the performance of BioPCM integration on both energy use and local occupant thermal sensation levels. Besides the presentation of heating and cooling loads, PMV values, and heat storage rates, descriptive statistical analysis, consisting of mean, minimum, and maximum, was conducted to quantify the variations among scenarios and support the robustness of the comparative results.

Zone Total Heating-Cooling Rates

The alternatives' heating and cooling rates were calculated for the November transition and the August hottest period reference days when the heating and cooling systems were active. The scenarios can be compared in terms of optimizing minimal energy consumption and achieving optimal climatic comfort conditions by selecting those that consume the least energy while still providing PMV values that indicate at least slight thermal stress for the two reference day conditions.

Lower cooling rates are obtained with calculations for all the alternatives compared to the reference alternatives between 11:00 and 18:00 on the August reference day. The highest energy consumption occurs at 14:00 with b-[nopcm-ins], while the lowest is with b3-[W-Pcm-ins] at 17:00. All the PCM-integrated walls and roof configurations dropped sensible cooling rates throughout the day. The alternative, b5-[roof-pcm-ins], provided the highest reduction of sensible cooling rate between 11:00-16:00. The Lowest reduction occurred with scenario b-[nopcm-ins] between 13:00-18:00. All the alternatives created lower PMV values than the reference alternative between 14:00 and 19:00. All the PMV values are out of the comfort range changing between 0.7 and 1.64. Therefore, lower PMV values occur for non-occupancy hours. However, b5-[roof-pcm-ins] provides the lowest PMV values throughout 11:00-18:00 among all the reference alternatives. PMV values of other scenarios with PCM generate similarity during the daily cycle (Fig. 8a).

Lower heating rates are calculated with the alternatives except for b1-[S-pcm-ins] and b4-[Part1-pcm-ins] compared to the reference alternatives between 06:00 and 19:00 on the November reference day. The highest energy consumption occurs with b1-[S-pcm-ins] between 06:00-10:00. All the PCM-integrated walls and roof configurations except b1-[S-pcm-ins] and b4-[Part1-pcm-ins] decrease the sensible heating rates throughout the day. All the alternatives create higher PMV values than the reference alternative until 1700. Lower PMV values occur with b1-[S-pcm-ins] than all alternatives. It also creates lower PMVs than the reference scenario after 17:00 (Fig. 8b). Since indoor temperatures are high at noon, there is no heating load with scenarios with PCM on the west and east walls, but with the b2-[E-pcm-ins] scenario, peak PMV values up to 0.84 are obtained. b5-[roof-pcm-ins] creates a small heating load at 10:00.

PMV Thermal Stress

Analyses considering the effects of interventions on buildings to increase the indoor thermal comfort of the occupants rely on performance indicators such as predicted mean vote index (PMV), Discomfort Index (DI), cooling power index (CPI), and Standard effective temperature (SET) index. Adilkhanova et al. (2021) used the "Total Discomfort Change" based on the sum of the reduction and increase among discomfort index levels for the specified hours for each level of discomfort. The discomfort level was calculated for the alternatives with and without PCM to examine the PCM performance only for the summer period. Indexes such as the Discomfort Index (DI) and Wet Bulb Globe Temperature (WBGT) are widely used to determine the sensation of heat stress levels in indoor areas. (Ghani et al. 2021, Adekunle and Nikolopoulou 2019). The "discomfort Index" (DI) presents the heating stress of the occupants in a zone by considering the wet and dry bulb temperatures in a zone (Eq. 5).

$$DI = 0.5(T_d + T_w) \quad (5)$$

DI presents data on the overheating risk of occupants during the cooling period, indicating moderate conditions between 24-28 ^{0}C and severe discomfort above 28 ^{0}C. DI values under 22 ^{0}C present no thermal discomfort conditions (Adilkhanova et al., 2021). Occupants may also feel dissatisfied with cold stress. However, DI highlights occupant discomfort; it does not consider cold stress. In this study, DI validated moderate conditions during occupancy hours, yielding similar results to the predicted mean vote (PMV) thermal stress results. According to this similarity, Predicted Mean Vote (PMV) thermal stress comprehensively evaluates summer, winter, and shoulder month conditions. Matzarakis et al. (1999)

presented ranges of the thermal indexes predicted mean vote (PMV) regarding the physiological (°C) thermal perception stress level. Scale changes among -3.5 and 3.5 PMV values. -0.5 – 0.5 refers to ideal conditions (Table 3).

This study investigates the impact of PCM on the thermal comfort conditions at different locations inside the zone through the PMV index for November and August reference days, and occupied hours. PMV values, calculated by Energyplus, rely upon a continuous comfort scale instead of standard discrete scale values (Energyplus, 2022). The study compares the total PMV thermal stress levels in 9 locations for the scenarios. PMV maps of Zone 2 present PMV variations of the scenarios for different time intervals of 01:00-08:00, 09:00-11:00, 12:00-13:00, 14:00-17:00, and 18:00-24:00 for the hottest and transition period reference days.

Table 3. Physiological stress levels. (Matzarakis et al. 1999)

PMV range		*Thermal Sensation*	*Physiological stress level*
-3.5	-2.51	Very cold	Extreme cold stress
-2.5	-1.51	Cold	Strong cold stress
-1.5	-0.51	Cool	Moderate cold stress
-0.5	-0.1	Slightly cool	Slight cold stress
0		Comfortable	No thermal stress
0.1	0.5	Slightly warm	Slight heat stress
0.51	1.5	Warm	Moderate heat stress
1.51	2.5	Hot	Strong heat stress
2.51	3.5	Very hot	Extreme heat stress

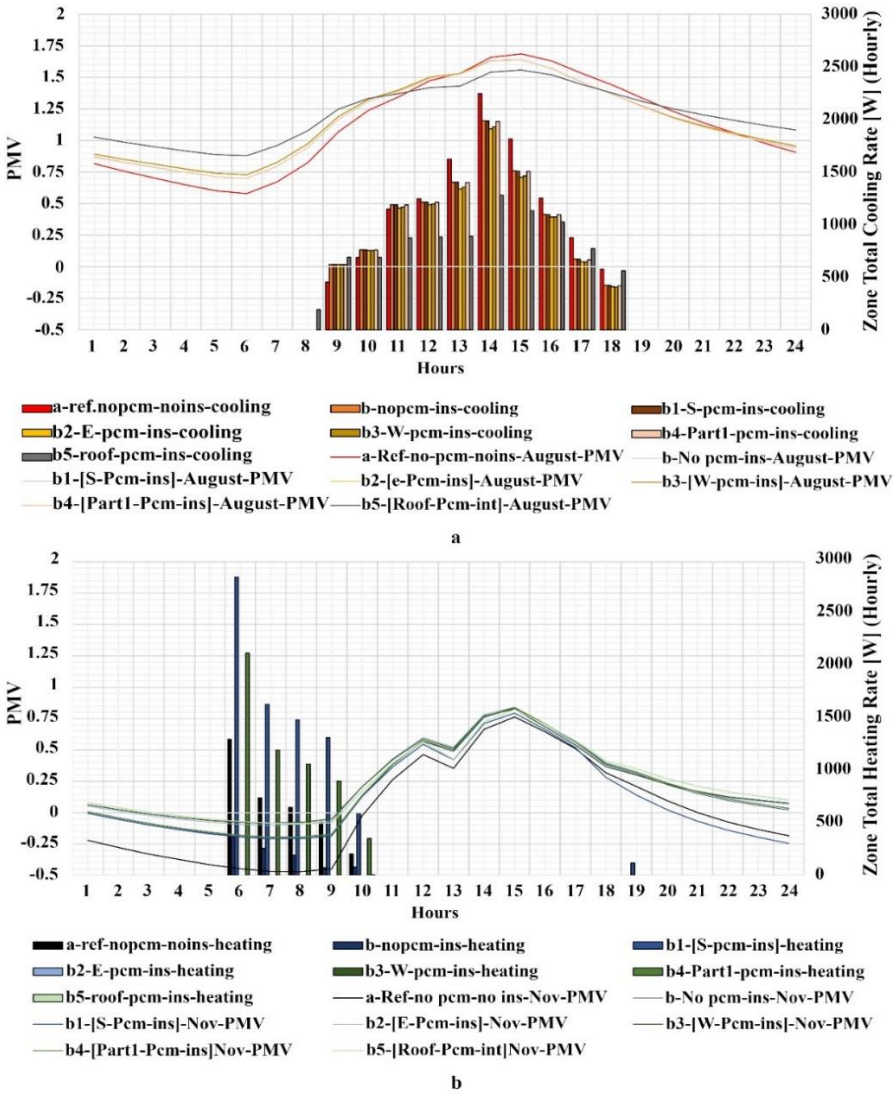

Fig. 8. a-Total cooling rate and PMV variations at location c2 in August, hottest, and b-Total heating rate and PMV value variations at location c2 in the transition period reference days.

PMV Variations at Different Locations in the Zone on the November Reference Day

PMV distribution map shows that for all time intervals of November reference day, predicted mean vote-PMV, representing the microclimatic comfort sensation of the occupants, changes between '-0.48-0.57 mean values when the heating system is off during occupancy hours (Fig. 9). It may be necessary to use heating during some hours in November. The selection of alternatives that provide higher operative temperatures without creating PMV values over 0.5 is more beneficial, considering the heating load reduction. For all the scenarios, including the reference alternative, 'a- [Ref-no PCM-no ins], PMV values increase to a maximum of 0.5 until 16:00. PMVs vary uniformly among the 9 locations for all periods. PMVs increase homogeneously in the zone until 17:00 and then decrease. A slight difference between the alternatives occurs at each time interval. The highest PMVs of 0.72 and 0.64 occur between 14:00 and 17:00, excluding the reference scenario. The alternative, b4-[part1-PCM-ins], creates a lower mean PMV and operative temperature distribution than the other scenarios during 09:00 and 11:00. The alternatives, b2-[E-Pcm-ins], b3-[w-pcm-ins], and b5-[roof-PCM-ins] between 09:00 and 11:00, create higher PMVs than the reference alternative, 'a- [Ref-no

PCM-no ins], providing a slight heat sensation by the effect of PCM integration, also decreasing the heating loads. PMV distribution with the same alternatives, except b1-[S-Pcm-ins] and b5-[roof-PCM-ins], creates more heat stress at 12:00-13:00 with values over the 0.5 range. The minimum PMV value of 0.46 occurs with the alternative b1-[S-Pcm-ins] with an operative temperature of 22.88 ^{0}C at location w2. A maximum of 0.57 PMV and an operative temperature of 23.44^{0}C were constituted at location e2 with alternative b2-[E-Pcm-ins]. All PMV values are higher between 14:00 and 17:00 compared to all other time intervals at all locations in the zone. All alternatives create higher thermal stress conditions compared to the reference situation. The lowest mean PMV value of 0.64 and operative temperature of 23.65^{0}C occurs with the alternative b1-[S-Pcm-ins] at w2. The highest PMV value of 0.72 and operative temperature of 24.09 ^{0}C constituted for b4-[part1-PCM-ins] at location e2 (Table 4).

Table 4. Max.-min. Mean PMV-PPD and Op. Temperatures at specific locations for different time intervals.

November		*Location*	*Alternative*	*Mean PMV*	*Mean PPD (%)*	*OperativeTemp. (^{0}C)*
09:00-11:00	Max	e2	b2-[E-Pcm-ins]	0.19	27.92	21.53
	Min	w2	b1-[S-Pcm-ins]	0.07	27.67	20.87
12:00-13:00	Max	e2	b2-[E-Pcm-ins]	0.57	28.68	23.44
	Min	w2	b1-[S-Pcm-ins]	0.46	28.19	22.88
14:00-17:00	Max	e2	b4-[part1-PCM-ins]	0.72	28.94	24.09
	Min	w2	b1-[S-Pcm-ins]	0.64	28.59	23.65

PMV Variations at Different Locations in the Zone on the August Reference Day

A maximum of 0.5 PMV is acceptable, considering the cooling load reduction on the August reference day, representing the hottest period. The mean PMVs range between 1.19-1.65, creating thermal stress when the heating system is off through occupancy hours, 09:00-13:00 (Fig.10). The reference scenario produces lower PMV values and operative temperatures than the other scenarios except b5-[roof-PCM-ins]. Uncomfortable microclimate conditions for the occupants occur significantly during 14:00-17:00 for all scenarios, reaching a maximum of 1.65 PMV value for the reference alternative. PMVs of all the other scenarios also increase similarly until 18:00 and then decrease.

PMVs and operative temperatures are distributed uniformly among the 9 locations for all alternatives for each period. However, significant differences occur among the parameters over different time intervals. The lowest PMV occurs in the morning at 09:00-11:00 during occupancy hours, due to the effect of heat losses at night with lower outside temperatures. Therefore, night ventilation would decrease PMV values during the daytime. All the alternatives, including the reference alternative, do not present optimal thermal comfort conditions during this period. The minimum mean PMV in the zone is 1.27, and the operative temperature is 27.67 ^{0}C at location w2 with b4-[Part1-Pcm-ins] during 09:00-11:00, while the maximum PMV is 1.33, and the operative temperature is 27.91 ^{0}C for b5-[Roof-Pcm-ins] at e2. Inversely, during 12:00-17:00 b5-[Roof-Pcm-ins] generates lower PMVs at all locations in the zone with a minimum of 1.41 and an operative temperature of 28.18 ^{0}C at location w2. Maximum PMV and operative temperatures for all alternatives occur at c2 between 12:00 and 17:00. The highest PMV of 1.59 occurs with b-No PCM-ins between 14:00 and 17:00. All the scenarios create lower PMVs than the reference alternative, still creating unsatisfactory conditions between 14:00 and 24:00 (Table5).

Results of Physiological Stress Grades Under Thermal Conditions Across Locations

According to the results for the hottest reference day, moderate thermal stress is the most-felt sensation at all locations in the zone for all the alternatives. The alternative b5-[Roof-Pcm-ins] causes the highest moderate stress and the lowest strong heat stress effect at all locations except c2, in the zone most of the time. At locations w1, w2, and w3, the "strong heat stress" effect is less than at the other locations for the same alternative. The "strong heat stress" is the most common sensation with the reference alternative for all the locations. All the other options reduce the amount of "strong heat stress" hours to moderate, with the most with alternative b5-[Roof-Pcm-ins]. There is either "Slight heat stress" or “no thermal stress” during occupancy hours at all locations for the alternatives.

There are significant differences in thermal stress levels among separate time intervals. Thermal sensation variations of the occupants are high during occupancy due to the interior temperature oscillations in August. The impact of BioPCM is observed directly at point e2. BioPCM in the eastern and western walls and the partition slightly increases the heat stress to strong in b3-[W-Pcm-ins] and b4-[Part1-Pcm-Ins] scenarios. There was no significant variation in thermal sensation between 09:00 and 12:00. All the alternatives created a higher level of thermal stress than the reference alternative, with few differences. An ignorable amount of variation in heat stress constitutes all the alternatives among the 9 locations. “Slight heat stress” is the highest level of sensation that occurs during the day after the “Moderate heat stress” sensation, with the alternatives for the November reference day.

Table 5. Max.-min. Mean PMV-PPD and Op. Temperatures at specific locations for different time intervals.

August		*Location*	*Alternative*	*Mean PMV*	*Mean PPD (%)*	*Operative Temp.(^{0}C)*
09:00-11:00	Max	e2	b5-[roof-PCM-ins]	1.33	41.96	27.92
	Min	w2	b4-[Part1-Pcm-ins]	1.27	38.91	27.67
12:00-13:00	Max	e2	b3-[W-Pcm-ins]	1.53	52.67	28.68
	Min	w2	b5-[roof-PCM-ins]	1.41	46.29	28.19
14:00-17:00	Max	e2	b-No PCM-ins	1.59	51.47	28.94
	Min	e1	b5-[roof-PCM-ins]	1.51	56.12	28.59

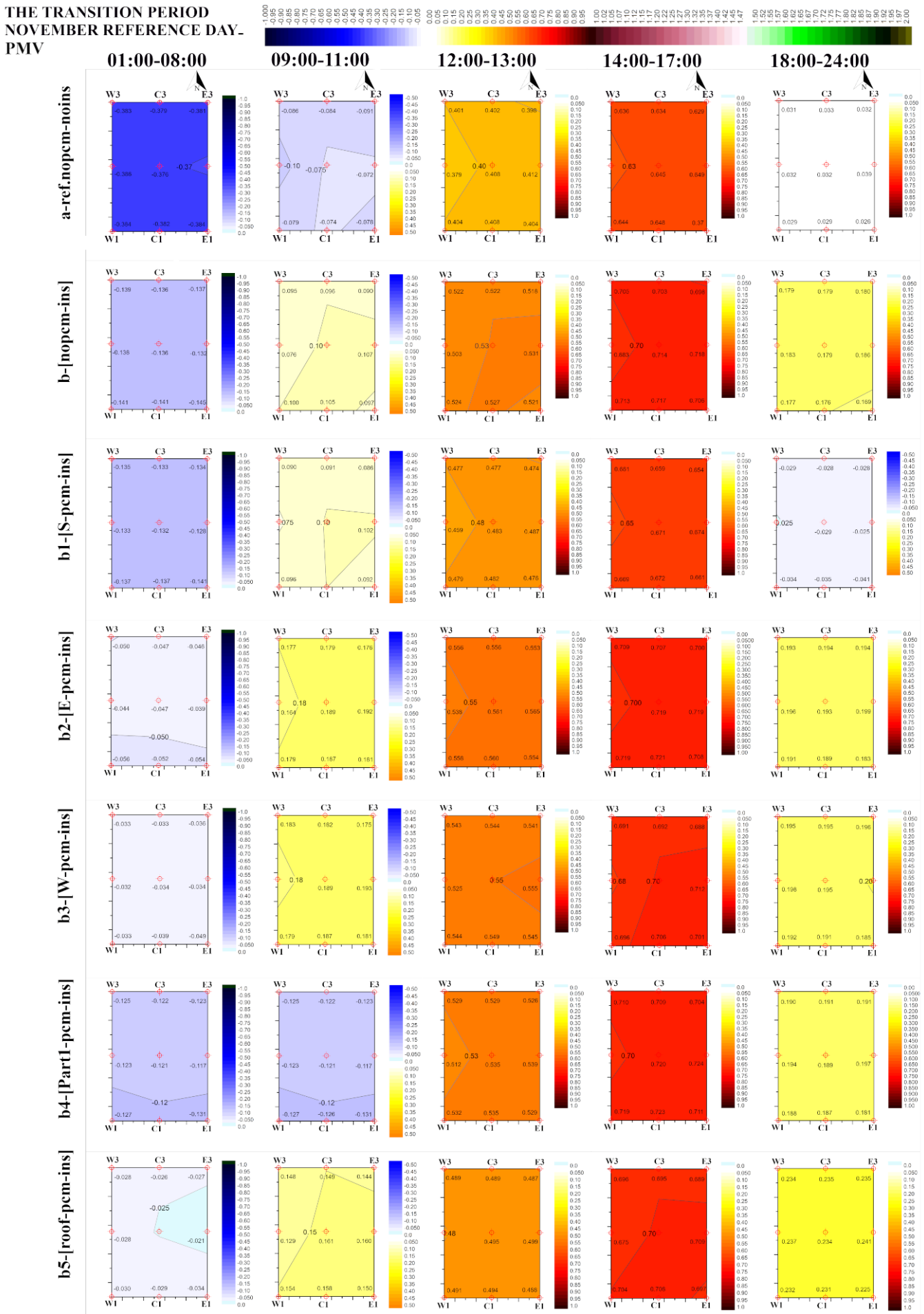

Fig. 9. PMV value variation at 9 locations in the atelier building on the November reference day.

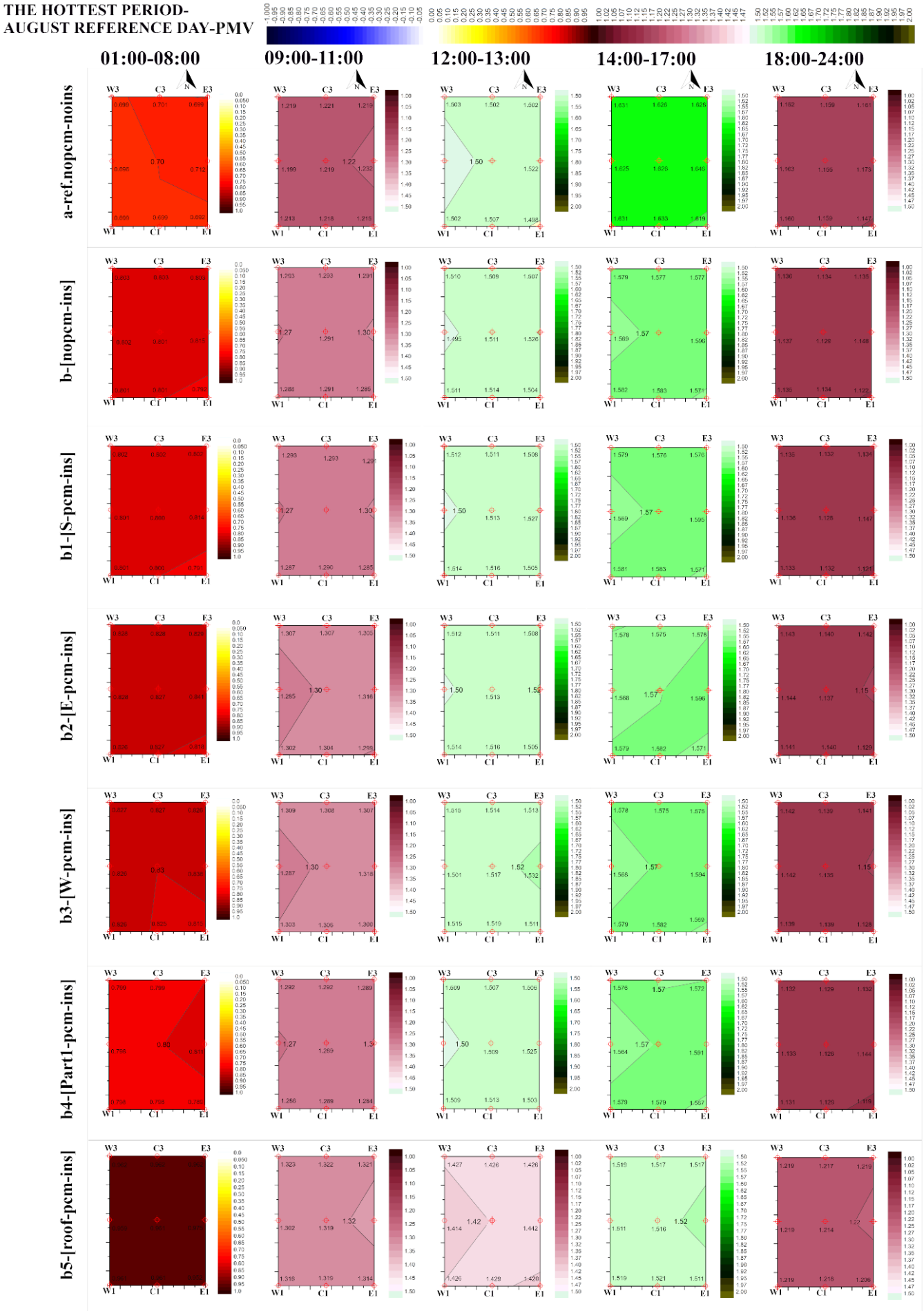

4321"

Fig. 10. PMV value variation at 9 locations in the atelier building on the August reference day.

The addition of insulation increased "Moderate heat stress" hours at all the locations. The highest moderate heat stress was observed at all locations with the b2-[E-Pcm-ins] scenario with PCM on the East facade. This rise occurs with b3-[W-Pcm-ins] at w3, c3, e3, and c2, e2 locations close to the Northern partition wall. With the addition of BioPCM, "Moderate heat stress" hours decreased at the w3 point with the b5-[Roof-Pcm-ins] scenario below the reference state. However, moderate cold stress occurred in the same location with daily temperature oscillation. Although this situation is also noted with scenario b1-[S-Pcm-ins] at the locations w3, w2, c3, and e3, these do not fall below the reference situation. The highest total of slight and non-thermal stress hours occurs with the b1-[S-Pcm-ins] scenario at all the locations. "Moderate heat stress" is higher in the afternoon hours between 14:00 and 17:00.

The total for August and November design days is calculated by assigning a higher weight to the "no thermal stress" and "slight thermal stress" options for all locations separately to compare the alternatives' benefits in providing thermal comfort conditions most of the time in a day. The total number of "no thermal stress" and "slight thermal stress" hours for the August reference day is zero for all locations in the zone (Fig. 11). Therefore, November reference day totals are dominant in the calculation. b-Nopcm-ins, b1-[S-Pcm-ins], and b3-[W-Pcm-ins] are the leading alternatives providing optimal thermal comfort conditions through most of the hours at location w2. b1-[S-Pcm-ins], generates the highest number of comfort conditions at w2, w3, c3, e3 compared to other alternatives except reference alternative. The scenario, b5-[Roof-Pcm-ins], provides the highest number of optimal comfort conditions at location w3. The b2-[E-Pcm-ins] configuration resulted in the fewest optimal thermal stress condition hours for all the locations. None of the alternatives provides a higher amount of non-thermal stress conditions than the reference alternative at any location in the zone. However, alternative b1-[S-Pcm-ins] yields PMV values closer to the reference alternative.

"Non-thermal stress" hours are much higher in November than in August, reference day conditions. BioPCM had a discernible impact on indoor comfort conditions, creating a microclimatic environment that carried some thermal stress risk for the occupants during the August reference day. Although the level of risk was not significant, the integration of BioPCM also led to conditions that were less comfortable than the reference alternative without BioPCM on the November reference day. Only b1-[S-Pcm-ins] provided a higher total of "no thermal stress" and "slight thermal stress" hours than b-No-PCM-ins with only insulation on the November reference day (Fig.12).

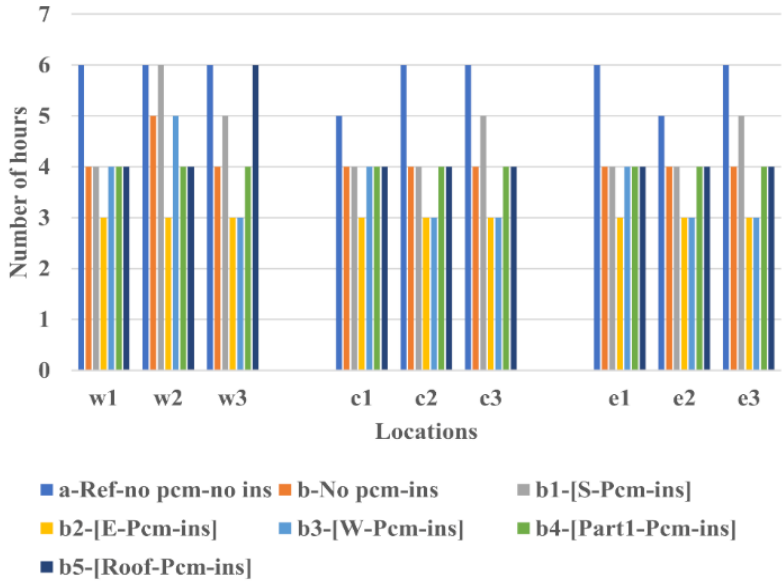

Fig. 11. Total "No thermal stress" and "Slight thermal stress" hours in August and November

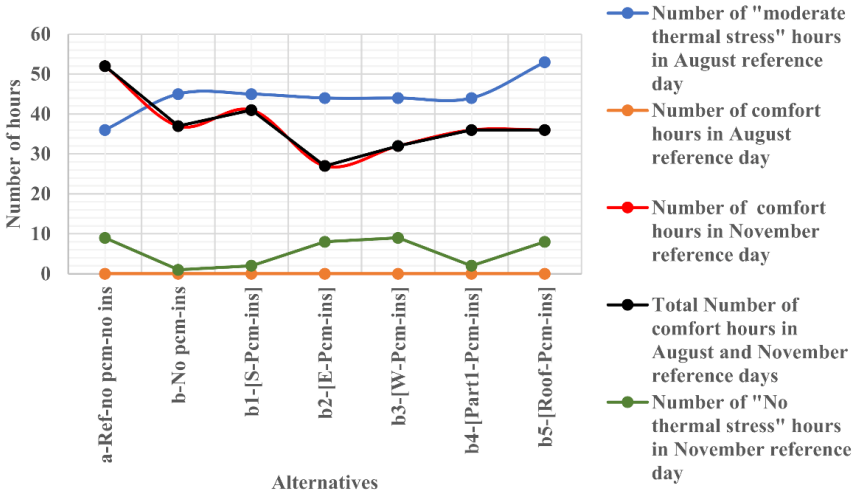

Fig. 12. Total number of comfort hours for each scenario at all locations

Scenario Comparison Based on Total Heating-Cooling Rates and Thermal Stress Grades

All values were normalized to holistically compare the performance of the scenarios in reducing the total hours of Moderate-strong heat stress, increasing the "no thermal and slight cold-heat stress" hours, and reducing heating-cooling loads on the hottest and transition period reference days with Min-max normalization equation, Eq. (6), where x' presents the normalized value, x is the original value and x min is the minimum value, and x max is the maximum value.

$$x' = \frac{x - x_{min}}{x_{max} - x_{min}} \quad (6)$$

Providing optimal thermal comfort conditions is the initial consideration in advancing energy efficiency within buildings (Oral & Yılmaz, 2002). Therefore, 60% of the cumulative values associated with thermal comfort criteria are assigned a greater weight, while the reduction of heating and cooling demands criteria has a complementary weight of 40%. This prioritization framework emphasizes the primary role that thermal comfort plays in the overarching objective of enhancing energy efficiency within built environments (Table 6). Moreover, the data from both the November and August reference days were considered in assessing thermal stress and heating-cooling loads. Notably, while scenario b5-[Roof-Pcm-ins] emerged prominently in August due to its efficacy in mitigating the "strong" heat stress, it is imperative to acknowledge that none of the alternatives provided conditions of "no thermal stress" or only "slight heat stress" during this period.

Table 6. Comparison of scenarios with normalized values

	Number of "Moderate heat stress" hours in August reference day	**Number of "Strong heat stress" hours in August reference day**	**Total Number of "No thermal and slight heat-cold stress" hours in the August reference day**	**Number of "Moderate heat stress" hours in the November reference day**	**Total Number of "No thermal and slight heat-cold stress" hours in the November reference day**	**TOTAL**	**Total Heating Loads**	**Total Cooling Loads**	**TOTAL**	**NET TOTAL**
	60%						40%			
	Lowest -1	Lowest -1	Highest -1	Lowest -1	Highest- 1		Lowest- 1	Lowest -1		
a-Ref-no Pcm-no ins	1	0	0	1	1	**1.8**	0.57	0.00	**0.23**	**2.03**
b-No Pcm-ins	0.47	0.53	0	0.4	0.4	**1.08**	0.88	0.36	**0.49**	**1.58**
b1-[S-Pcm-ins]	0.47	0.53	0	0.56	0.56	**1.27**	0.00	0.36	**0.14**	**1.42**
b2-[E-Pcm-ins]	0.53	0.47	0	0	0	**0.6**	1.00	0.47	**0.59**	**1.19**
b3-[W-Pcm-ins]	0.53	0.47	0	0.2	0.2	**0.84**	1.00	0.45	**0.58**	**1.42**
b4-[Part1-Pcm-ins]	0.53	0.47	0	0.36	0.36	**1.03**	0.30	0.37	**0.27**	**1.29**
b5-[Roof-Pcm-int]	0	1	0	0.36	0.44	**1.08**	1.00	1.00	0.8	1.88

Therefore, comparative analyses for the August reference day may be inherently limited in significance. Consequently, the transition period-reference day results possessed a dominant role in comparison across all scenarios due to the achievement of optimal thermal comfort conditions primarily, and then heating-cooling load reduction performance, regardless of seasonal variations. According to the comparison of the sums of the parameters for thermal stress, there was no alternative with a higher value than the reference alternative. While the conditions most closely approximating the reference scenario were achieved with b1-[S-Pcm-ins] and b3-[W-Pcm-ins], the most unfavorable conditions occurred with b2-[E-Pcm-ins]. However, b3-[W-Pcm-ins] was insufficient in providing the total number of "No thermal and slight heat-cold stress" hours on the November reference day compared to b1-[S-Pcm-ins].

DISCUSSION

Optimization of energy consumption reduction for heating and cooling and thermal comfort in buildings requires prioritizing the achievement of interior comfort levels among operative temperature ranges that users will feel satisfied with (Evola et al., 2013; Oral and Yılmaz, 2002). Due to the Melting-freezing temperature range, thickness, implemented surface area, and the amount characteristics of materials, such as BioPCM, applied to building components, energy consumption may not be reduced at different time intervals depending on the climatic and environmental conditions of the building's location and acceptable levels of user satisfaction may not be achieved at each location in all time intervals in the spaces. This simulation study considers the impacts of M182/Q23 BioPCM, selected due to its low adverse environmental effects and appropriate melting-freezing temperature values based on literature data and the properties already defined in the DesignBuilder database when applied to

different building components on total heating-cooling rates and local thermal sensations of occupants in a zone. Although the model was calibrated and validated against measured data, specific simplifications, including using a basic enthalpy-temperature model, closed window approach, and a fixed BioPCM integrated surface area for each scenario, introduce uncertainties, limiting the exact quantitative accuracy of the results. These assumptions were necessary to observe the variations among the scenarios. However, the observed trends and the variations among the results provide reliable insights for evaluating BioPCM applications. The following sections detail the variations.

Heating and Cooling Rates and Thermal Comfort Variations with BioPCM

Unlike many studies that consider PCM application to entire building envelopes or focus solely on peak climatic conditions, this study uniquely isolates the effects of individual BioPCM-integrated building components with identical surface areas under the hottest and transitional periods. This approach provides a detailed evaluation of localized thermal sensation variations of occupants, as well as diurnal, heat flow, and storage dynamics for individual building components, which are often underrepresented in the literature.

This simulation-based study calibrated with measurement data revealed that BioPCM reduced the total cooling loads during the hottest period reference day with all scenarios, decreasing PMV values but without a significant positive effect on thermal comfort with high operative temperatures. In some studies, such as those by Qu et al. (2021), PCM is beneficial in meeting energy consumption reduction criteria and thermal comfort enhancement. In contrast, in some, such as the study of Staszczuk and Kuczynski (2021), PCMs were beneficial in mitigating energy consumption but insufficient in providing user comfort, similar to this study. The study of Qu et al. (2021) validated the simulation results by demonstrating a similar energy consumption reduction of 11.9% in a building in a region with temperate climatic conditions and the same type of BioPCM during the summer period. In the study, thermal comfort conditions were increased by the effect of PCM. Deterioration of thermal comfort conditions from the study by Qu et al. (2021) refers to the differences among parameters such as climatic conditions, PCM-applied surface areas, and simulation assumptions in the two studies.

The survey by Staszczuk and Kuczynski (2021) and Kuczynski and Staszczuk (2020) detecting temperature exceedances above comfort thresholds among indoor measured data for the zone with PCM integrated on the interior surfaces of the building envelope in Poland with temperate climate conditions highlighted that the integration of PCM into interior surfaces was similarly insufficient to improve thermal comfort in environments with low-temperature fluctuations. Due to high interior temperatures, PCM could not solidify, which limited its effectiveness in enhancing comfort conditions, similar to the August reference day simulation results in this study.

In all alternatives with BioPCM in the indoor environment, the internal operative temperatures are in the range of 25.35-28.90 ^{0}C, and the interior surface temperatures are in the range of 25.57 -28.93 ^{0}C, revealing that BioPCM cannot change from liquid to solid due to high internal operative and surface temperatures. In this process, PCM's low conductivity and insulation properties came to the fore rather than its latent heat storage properties. However, since the indoor temperatures were high, the BioPCM layer prevented more heat from escaping to the outdoors, causing the indoor space to warm up more. The findings on cooling and heating rates with BioPCM lead to determining its pivotal role in different building components, such as roofs, differently oriented outer walls, and interior partitions.

Effects of Different Building Components with BioPCM

Total cooling rates with BioPCM-applied scenarios of the external walls and the partition were similar. However, the roof application created a lower cooling rate, a significant finding, as the bioPCM-applied surface area was the same for all scenarios.

Roofs, being structural components, are more susceptible to the effects of solar radiation. Despite the intense solar temperature affecting the roof surface, on August reference day, the lower interior surface temperatures may be due to the sensible heat storage of BioPCM M182/Q23 in the liquid phase after fully melting rather than latent heat storage (Fig. 13). The liquid BioPCM layer effectively prevented the temperature from rising rapidly with sensible heat storage, although not as much as in the conditions in which the PCM phase change process was active. However, the BioPCM's capability to store additional heat decreased as the solar temperature rose. PCM, which also has low conductivity in the liquid state, slowed heat transfer. This effect occurs in the roof areas where PCM is applied compared to partial roof areas with only insulation. Roof surfaces with only insulation experience a rapid temperature increase as sensible heat storage dominates. The notification of Figueiredo et al. (2017), Bohorquez-Ordenes et al. (2021), Qu et al. (2021), and Saffari et al. (2015) on PCMs application to building components exposed to intense solar radiation, enhancing heat storage and dampening temperature oscillations, and improving thermal comfort shows significance in this study with BioPCM application on the roof.

On the transition reference day, solar radiation and occupancy periods significantly affect the thermal behaviors of the east and west walls and the roof with BioPCM (Fig. 14). For the east wall, solar radiation from 9:00-12:00 raises the surface temperature to PCM's melting temperature, causing it to absorb latent heat. However, indoor operative temperatures rise during this melting phase, with occupancy occurring during morning hours, indicating that sensible heat storage also occurs. At noon, during the break time, heat storage decreases. As occupancy begins again, sensible heat storage becomes dominant until the heat transfer shifts from the interior to the exterior surface as the outside temperatures drop, albeit more slowly, due to the low conductivity of PCM and insulation layers.

The west wall experiences a similar phenomenon, with solar radiation between 12:00 and 15:00, causing PCM to reach its melting point around 14:00, storing heat until the end of occupancy.

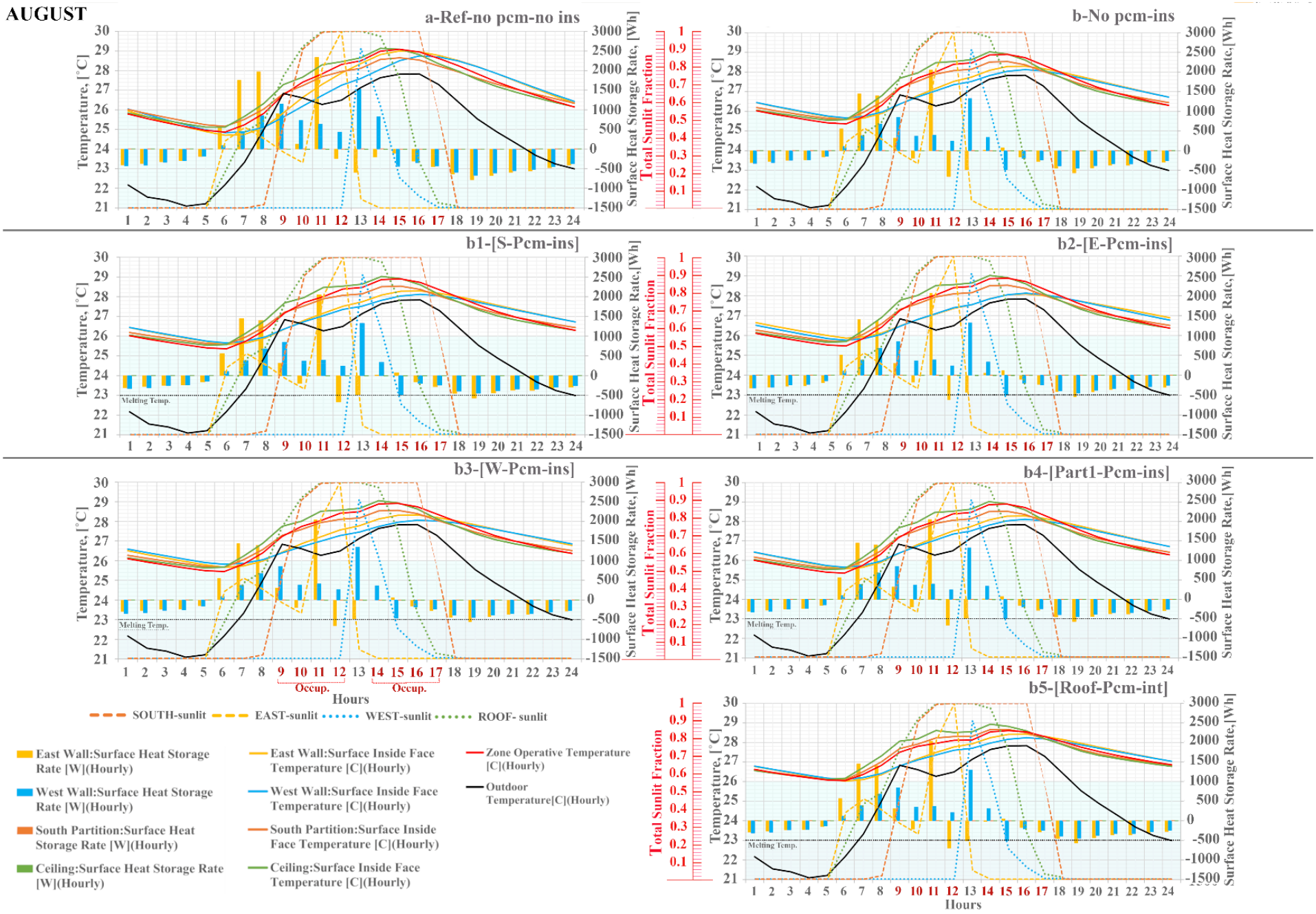

Fig. 13. Daily variation of total heat storage rates and surface temperatures of the outer walls on the August reference day

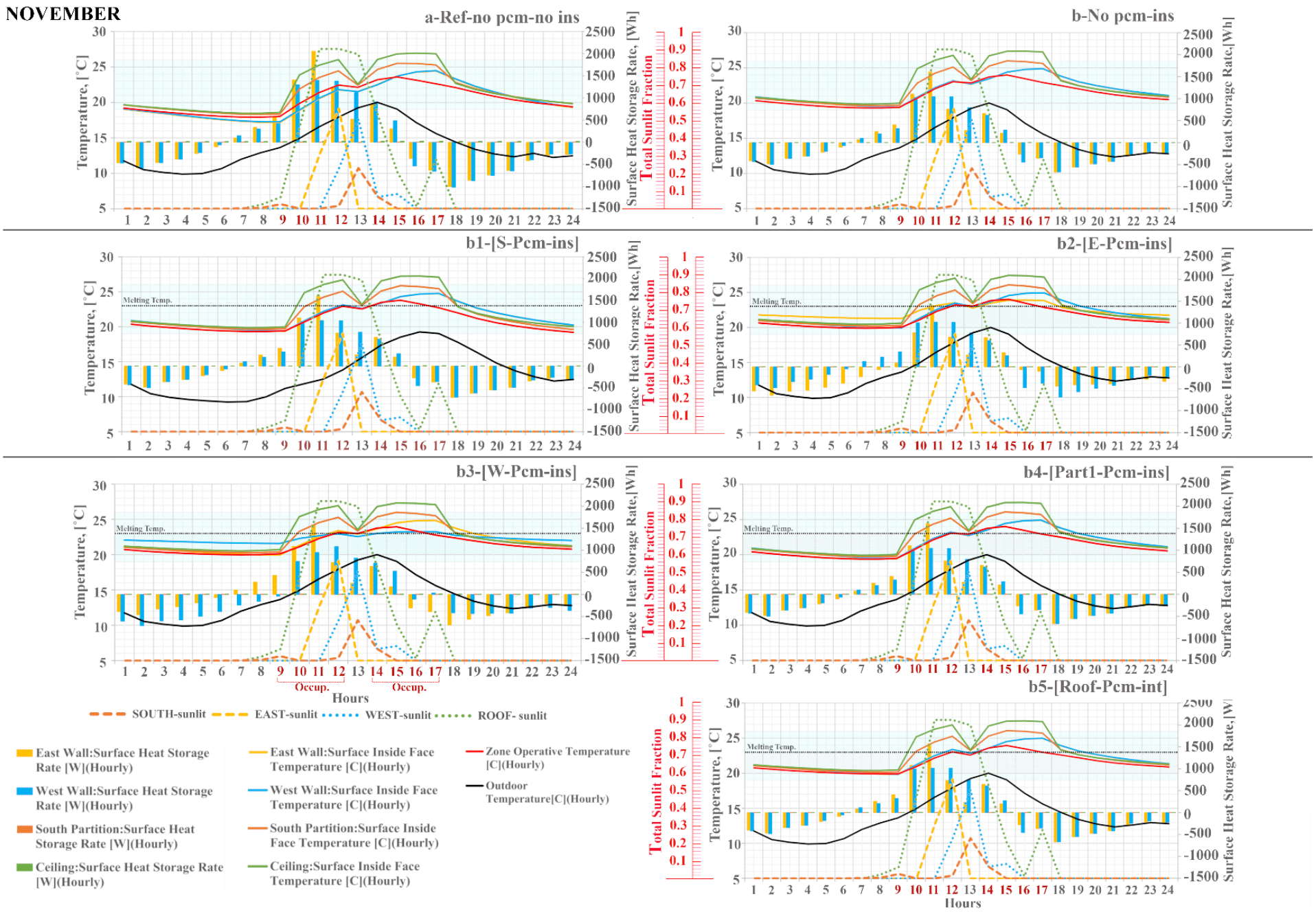

Fig. 14. Daily variation of total heat storage rates and surface temperatures of the outer walls on the November reference day

As external temperatures decrease, heat transfer occurs slowly with the effect of BioPCM and the insulation layer from the interior to the exterior surface. Unlike the walls, the roof accumulates heat throughout the day, with peak storage between 10:00 and 13:00 due to prolonged solar radiation and occupancy. When the occupancy ends, the roof shows a reduction in surface temperature. However, positive heat storage values indicate heat transfers to the exterior surface, and the stored heat remains sensible. Nonetheless, the PCM and insulation layers slow down this heat transfer due to their low conductivity.

Local Thermal Sensation Variations with BioPCM

During the hottest period reference day, the impact of BioPCM was more noticeable after 14:00, leading to slightly lower PMV values than the reference case. In the transition period, PMV values varied significantly across different times of the day, with the highest thermal stress occurring between 14:00 and 17:00. Incorporating short-term morning ventilation could optimize thermal stress without increasing cooling loads.

Heat storage variations significantly affect these thermal comfort conditions. BiopCM application on different building components in each scenario presented critical diurnal heat storage dynamics at specific hours, such as 09:00, 10:00, 14:00, and 18:00. The occupancy situation and the effects of solar radiation significantly affected heat storage in the walls, especially when using PCMs that undergo phase transitions during the day—non-occupancy periods, particularly at 14:00, 10:00, and 18:00, led to a notable decrease in heat storage among all the alternatives. One hour before had a noteworthy effect on heat storage, significantly reducing all other options, particularly at 14:00, followed by 10:00 and 18:00.

The southern façade with BioPCM in the b2-[E-Pcm-ins] scenario does not directly interact with the primary zone due to the buffer area. Therefore, the effect of BioPCM, which causes critical thermal sensation changes at the reference points, can be best observed on the east or west facades, directly exposing the outdoor environment and the zone. Due to the high PMV values at the close reference locations, the study examines diurnal heat storage, interior and exterior surface conduction, convection, and solar radiation heat gain, and loss variations on the Eastern wall in the alternatives b2-[E-Pcm-ins], b1-[S-Pcm-ins], b-No Pcm-ins, a-Ref-no Pcm-no ins for the specific hours of the transition period reference day. These simultaneous heat transfer and heat storage variations for the scenarios selected for detailed analysis, due to their distinct performance in terms of energy consumption reduction and thermal comfort levels in both August and November reference days, are presented in Figure 15 and 16.

On the transition period reference day, occupants did not experience heat stress except between 14:00 and 17:00 when PCM or insulation was not applied. Adding insulation increased daytime operative temperatures and reduced heating loads, but prolonged moderate heat stress in the afternoon. The PCM addition led to a predominant "moderate heat stress" sensation during midday and afternoon. PMV differences were distinct across all alternatives in the morning and early afternoon, including the alternative with only insulation [b-No-pcm-ins]. The variation decreased with the alternative b1-[S-Pcm-ins] scenario at noon but remained higher than the reference condition without insulation and PCM. This increase can be considered positive in the context of energy efficiency, up to the point where it creates moderate heat stress in November reference day conditions. These thermal sensation variations directly interact with the heat storage phenomenon in different alternatives. The effect of BioPCM and insulation layers on heat accumulation and dissipation from building components significantly affected local thermal comfort levels. Heat transfer rates on building elements are primarily governed by conduction, modulated by the thermal storage and the release processes of the BioPCM layer.

In the transition reference day conditions, when comparing the reference situation, a-ref-nopcm-noins with the b-[No pcm-ins] alternative, the insulation-only scenario, it becomes clear that insulation increases the interior surface and indoor operative temperatures by reversing heat transmission with convection at 09:00. Since the other alternatives with PCM also have insulation installed, the b-[Nopcm-ins] scenario can serve for comparison. At 09:00 and 10:00, with occupancy conditions, the lowest heat storage occurs in the case b2-[E-Pcm-ins], where BioPCM is on the East wall. BioPCM stimulates heat gain on the interior surface of the East wall by conduction. This results in rises in surface temperature, reinforced heat loss with convection, and higher interior operative temperatures. Significant PMV variations in the morning hours correspond to heat storage variations induced by the early heat accumulation caused by the BioPCM application on the East wall. As heat transfer predominantly occurs toward the inner surface, the interior surface temperature is the highest with the b2-[E-Pcm-ins] alternative. The radiant temperature is the highest in location e1 among the others on the same line near the E wall, still providing a slight heat stress level for the occupants. The walls with high heat storage demonstrated lower indoor surface temperatures during these times (Figure15).

As shown in Appendix A2, detailed heat transfer phenomena and radiant heat gain for b2-[E-Pcm-ins], b1-[S-Pcm-ins], b-No Pcm-ins, and a-ref-no Pcm-noins are presented for the specific hours. At 15:00, the heat storage of the East wall reached its highest with the b2-[E-Pcm-ins] alternative. That lowered interior surface temperature while decreasing indoor air temperature with decreased convective heat loss. A similar impact showed itself at 16:00, generating even lower interior surface temperatures than the reference condition. The surface Thermal Radiation Heat Gain Rate of the East wall with b2-[E-Pcm-ins] is higher than the other alternatives at 15:00 and 16:00, creating higher radiant temperatures at location e2 [Figure 16)]. The heat storage phenomena directly contributed to the moderate heat stress sensation in the afternoon, which underlines the connection between BioPCM location, façade orientation, and local thermal comfort. When heating was assumed to be active at 15:00, none of the alternatives resulted in any heating load. However, b1-[S-Pcm-ins] generated higher inner surface temperatures than the reference condition and lower temperatures than b-No PCM-ins. In the case of b1-[S-Pcm-ins], heat loss through conduction decreased, while heat transfer through convection increased toward the classroom zone.

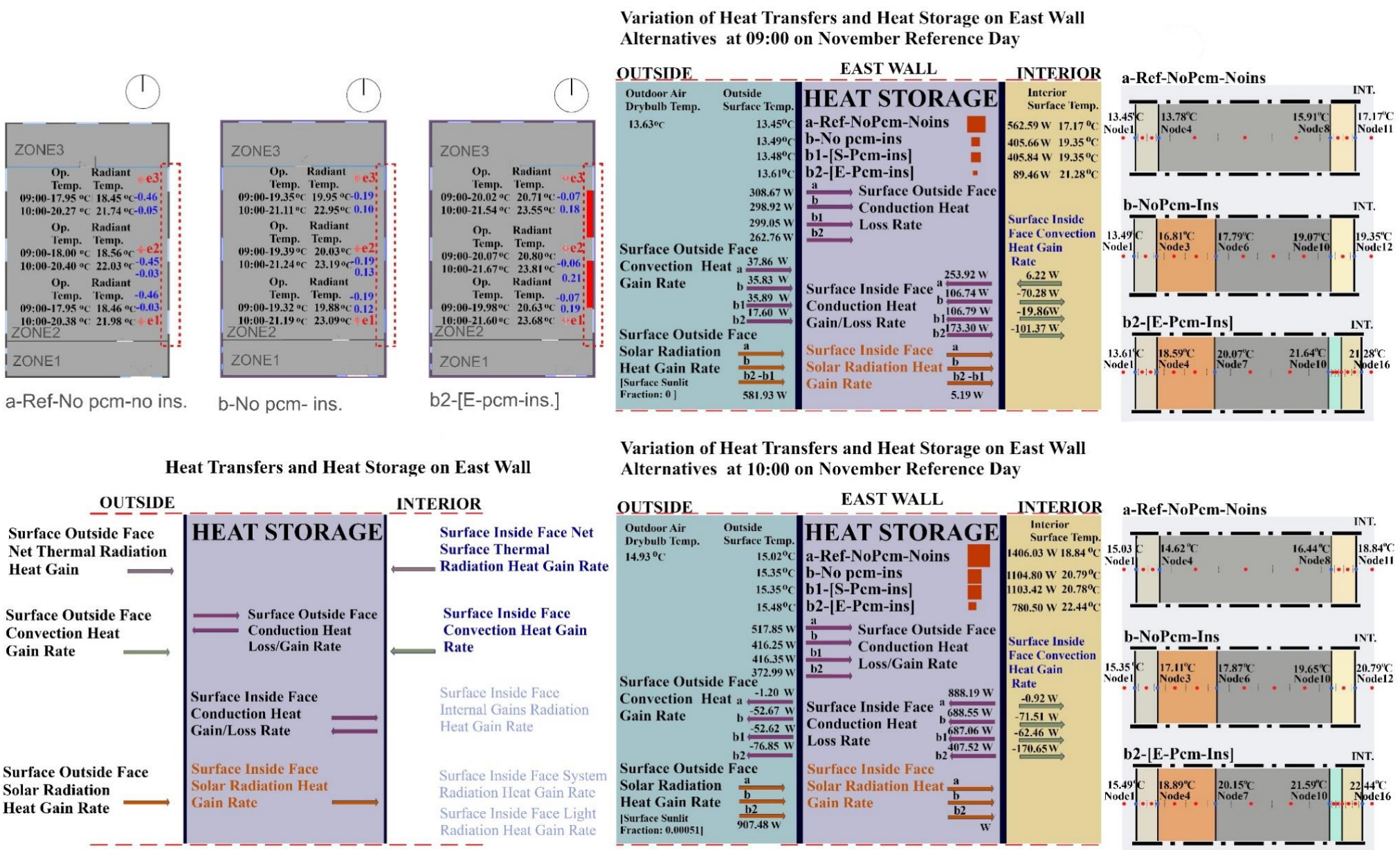

Fig. 15. Variation of heat transfers and heat storage on east wall alternatives at 09:00 on November Reference day

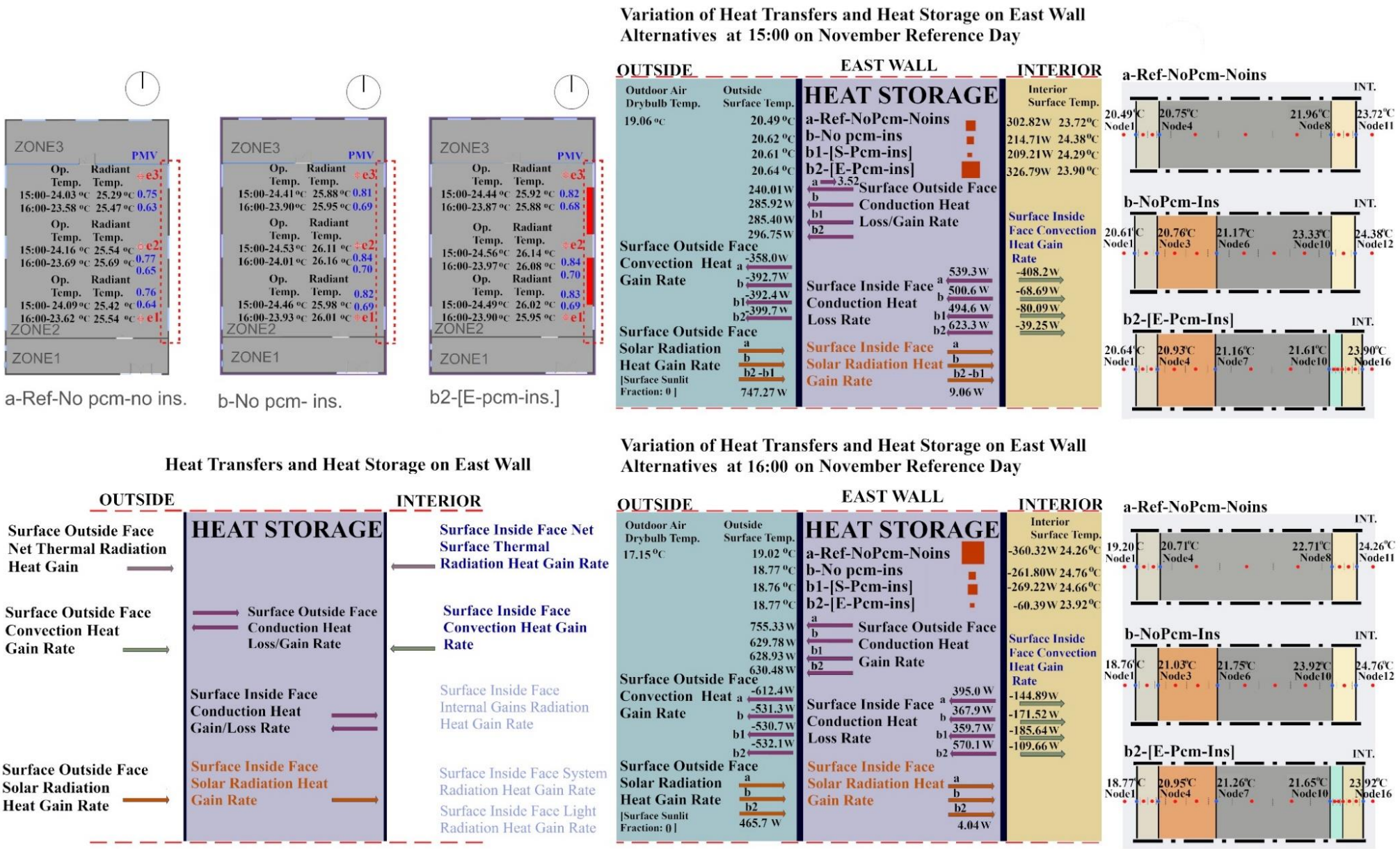

Fig. 16. Variation of heat transfers and heat storage on east wall alternatives at 15:00 on November Reference day

The differentiating effects of PCM-integrated walls and roofs in reducing energy consumption also affected thermal comfort conditions. However, this difference regarding its impact on thermal comfort conditions, primarily on the local thermal sensations of the occupants, did not create substantial changes. The BioPCM-applied surface area, assumed to be similar for each scenario for comparison, was insufficient to present the impact on the variation of local thermal stress. While BioPCM provided benefits in reducing energy consumption, its capability to effectively improve thermal comfort was limited during occupancy hours on both the hottest and transition period reference days, especially without night ventilation when the heating and cooling systems were inactive. This finding highlights the importance of integrating PCM applications with supplementary passive design solutions such as night and early morning ventilation.

CONCLUSIONS

According to the study, strategic PCM placement is essential to enhance building energy efficiency and thermal comfort in temperate climates, considering transition and peak periods. All scenarios mitigated cooling rates, with a maximum reduction of 25% achieved by the roof. The thermal behavior of building envelope components and interior partitions with PCMs varied notably. Roofs under prolonged solar radiation benefited from the capability of bioPCM to slow heat transfer, which is essential for reducing cooling loads. In contrast, BioPCM applied on East and West facades exhibited different performances, with heat storage and release affected strongly by timing, heat gains by occupancy, and intensity of solar exposure. In contrast, BioPCM applied on East and West facades exhibited different performances, with heat storage and release affected strongly by timing, heat gains by occupancy, and intensity of solar exposure. BioPCM-integrated East-West walls and the roof significantly reduced heating, with modest enhancements to thermal sensation.

Utilizing the selected BioPCM on different building elements yielded comparable thermal stress sensations at specific locations within the zone during distinct time intervals. However, the minor fluctuations observed in thermal perceptions among occupants at the nine interior locations facilitate the conduction of assessments concerning the central location in the zone. Notably, during the transition period, the highest PMV values were recorded near the East-central part of the zone, with BioPCM on the East wall. Scenarios were normalized and compared, prioritizing heat stress parameters. The South wall-BioPCM scenario scored highest due to the buffer zone effect among the outer and interior partition walls. The scenario with PCM implementation on the East wall consumed the least energy. Still, in terms of generating heat stress, it did not contribute to comfort in the same way as the others during the hottest period.

The adverse effect of BioPCM was most significant in the afternoon during the transition period, though less considered than in the hottest period. In both periods, the BioPCM-integrated roof is the leading scenario in terms of energy efficiency. However, it provided only slight improvements, less than the reference condition in the other scenarios, indicating that BioPCM alone may not ensure occupant comfort during these times. Although BioPCM-applied building elements decreased energy consumption, their capability to improve thermal comfort, especially during peak periods, was limited without supplementary strategies such as night or partial morning ventilation.

A crucial consideration was the assumption of a PCM amount equivalent to the respective facade area of the south with minimum area. The PCM-applied surface area of the building components was limited to create a notable variation in the localized indoor thermal sensation. Future research should consider designing building envelopes with more significant amounts of PCMs activated with ventilation strategies to optimize energy efficiency. Further studies using Typical Meteorological Year (TMY) data for energy consumption calculations and comfort range assessments without mechanical systems activation can further refine the findings.

REFERENCES

Adekunle, T. O., Nikolopoulou, M. (2019). Winter performance, occupants' comfort, and cold stress in prefabricated timber buildings. *Building and Environment*, 149, 220–240.

Adilkhanova, I., Memon, S. A., Kim, J., Sheriyev A (2021). A novel approach to investigate the thermal comfort of the lightweight relocatable building integrated with PCM in different climates of Kazakhstan during summertime. *Energy*, 217,119390.

Ahangari, M., Maerefat, M. (2019). An innovative PCM system for thermal comfort improvement and energy demand reduction in buildings under different climate conditions. *Sustain Cities and Society*, 44,120–129.

Alharbey, R. A., Daqrouq, K. O., Alkhateeb, A., et al. (2022). Energy exchange is achieved by inserting eco-friendly bio-phase change material into the vertical walls to make the buildings energy-efficient. *Journal of Building Eng*ineering. 56,104777.

Aridi, R., Yehya, A. (2022). Review the sustainability of phase-change materials used in buildings. Energy Conversion and Management: X,15,100237.

Baniassadi, A., Sailor, D.J., Bryan, H.J., et al. (2019). Effectiveness of phase change materials for improving the resiliency of residential buildings to extreme thermal conditions. *Solar Energy*, 188, 190–199.

Bejan, A. S., Catalina, T. (2016). The implementation of phase-changing materials in energy-efficient buildings. Case study: EFdeN project. *Energy Procedia*, 85, 52–59.

Berardi, U., Manca, M. (2017). The energy saving and indoor comfort improvements with latent thermal energy storage in building retrofits in Canada. Energy Procedia, 111, 462–471.

BioPCM. (2020) BioPCM data sheet Q23. Retrieved August 16,2024, from https://phasechange.com/wpcontent/uploads/2020/08/BioPCM-Data-Sheet-Q23.pdf.

Bohórquez-Órdenes, J., Tapia-Calderón, A., Vasco, D. A., et al. (2021). Methodology to reduce cooling energy consumption by incorporating PCM envelopes: A case study of a dwelling in Chile. *Building and Environment,* 206, 108373.

Cárdenas-Ramírez C., Jaramillo, F., Gómez, M., et al. (2020). A systematic review of encapsulation and shape-stabilization of phase change materials. *J Energy Storage*. 30, 101495.

Casini, M. (2016). Smart Buildings: Advanced Materials and Nanotechnology to Improve Energy Efficiency and Environmental Performance. Woodhead publishing. pp.179–216.

Costanzo, V., Evola, G., Marletta, L., et al. (2018). The effectiveness of phase change materials in relation to summer thermal comfort in air-conditioned office buildings. *Building Simul*ation,11(6),1145–1161.

De Masi, R. F., Gigante, A., Vanoli, G. P. (2020). Numerical analysis of phase change materials for optimizing the energy balance of a nearly zero energy building. *Sustainable Cities and Soc*iety, 63,102441.

Dincer, I., Rosen, M. A. (2011). Thermal Energy Storage: Systems and Applications. 2nd ed. United Kingdom: Wiley.

Evola, G., Marletta, L., Sicurella, F., et al. (2014). Simulation of a ventilated cavity to enhance the effectiveness of PCM wallboards for summer thermal comfort in buildings. *Energy and Buildings*, 70, 480–489.

Fabiani, C., Pisello, A. L., Barbanera, M., et al. (2020). Palm oil-based bio-PCM for energy efficient building applications: Multipurpose thermal investigation and life cycle assessment. *Journal of Energy Storage*, 28, 101129.

Figueiredo, A., Vicente, R., Lapa, J., et al. (2017). Indoor thermal comfort assessment using different constructive solutions incorporating PCM. *Applied Energy*, 208,1208–1221.

Ghani, S., Mahgoub, A.O., Bakochristou, F., et al. (2021). Assessment of thermal comfort indices in an open air-conditioned stadium in a hot and arid environment. *Journal of Building Engineering*, 40,102378.

Turkish State Meteorological Service. (2024). Heating and cooling degree days of Kocaeli. Retrieved April 9, 2024, from https://www.mgm.gov.tr/veridegerlendirme/gun-derece.aspx?g=merkez&m=41-00&y=2024&a=02.

Kuczyński, T., Staszczuk, A. (2020). Experimental study of the influence of thermal mass on thermal comfort and cooling energy demand in residential buildings. *Energy*., 195, 116984.

Kuznik, F., Virgone, J., Johannes K, et al. (2011). In-situ study of thermal comfort enhancement in a renovated building equipped with phase change material wallboard. *Renewable Energy*., 36(5), 1458–1466.

Matzarakis, A., Mayer, H., Iziomon, M. G., et al. (1999). Applications of a universal thermal index: Physiological equivalent temperature. *International Journal of Biometeorol*ogy, 43(2),76–84.

Nghana, B., Tariku, F. (2016). P hase change material (PCM) impacts buildings' energy performance and thermal comfort in a mild climate. *Building and Environ*ment, 99, 221–238.

Oral, G. K., Yilmaz, Z. (2002). The limit U values for building envelope related to building form in temperate and cold climatic zones. *Building and Environ*ment, 37, 117–125.

Qu, Y., Zhou, D., Xue, F., et al. (2021). Multi-factor analysis on thermal comfort and energy saving potential for PCM-integrated buildings in summer. *Energy and Build*ings, 241, 110966.

Raftery, P., Keane, M., Costa, A., et al. (2011). Calibrating whole building energy models: Detailed case study using hourly measured data. Energy and Buildings., 43(12), 3666–3679.

Rathore, P. K. S., Shukla, S. K. (2019). The potential of microencapsulated PCM for thermal energy storage in buildings: A comprehensive review. *Construction and Building Mater*ials, 225, 723–744.

Saffari, M., de Gracia, A., Ushak, S., et al. (2016). The economic impact of integrating PCM as a passive system in buildings using the Fanger comfort model. *Energy and Build*ings, 112, 159–172.

Socaciu, L. G. (2012). Thermal energy storage with phase change material. Leonardo Electronic Journal of Practices and Technologies, 11, 75–98.

Staszczuk, A., Kuczyński, T. (2021). The impact of wall and roof material on the summer thermal performance of the building in a temperate climate. *Energy,* 228, 120482.

Tunçbilek, E., Arıcı, M., Bouadila, S., et al. (2020). Seasonal and annual performance analysis of PCM-integrated building brick under the climatic conditions of the Marmara region. *Journal of Thermal Analysis and Calorimetry*, 141(1), 613–624.

Turkish Standards Institution. (2025). TS825: Thermal Insulation Requirements for Buildings. Ankara.

U.S. Department of Energy. EnergyPlus™ Version 22.1.0 Documentation. Engineering Reference. March 2022.

Vicente, R., Silva, T. (2014). Brick masonry walls with PCM microcapsules: An experimental approach. *Applied Thermal Eng*ineering, 67, 24–34.

Vik, T. A., Madessa, H. B., Aslaksrud, P., et al. (2017). Thermal performance of an office cubicle integrated with a bio-based PCM: Experimental analyses. *Energy Procedia*., 111, 609–618.

Wijesuriya, S., Brandt, M., Tabares-Velasco, P. C., et al. (2018). Parametric analysis of a residential building with phase change material (PCM)-enhanced drywall, precooling, and variable electric rates in a hot and dry climate. *Applied Energy*, 222, 497–514.

Yadav, A., Samykano, M., Pandey, A. K., et al. (2023). A systematic review on bio-based phase change materials. *International Journal of Automotive and Mechanical Eng*ineering, 20(2), 10547–10558.